New algorithm for detecting smaller retinal blood vessels in fundus images

Robert LeAnder*, Praveen I. Bidari
Tauseef A. Mohammed, Moumita Das, Scott E. Umbaugh
Department of Electrical and Computer Engineering, Southern Illinois University Edwardsville
Edwardsville, IL, USA, 62203-1801

ABSTRACT

About 4.1 million Americans suffer from diabetic retinopathy. To help automatically diagnose various stages of the disease, a new blood-vessel-segmentation algorithm based on *spatial* high-pass filtering was developed to automatically segment blood vessels, including the smaller ones, with low noise. Methods: Image database: Forty, 584 x 565-pixel images were collected from the DRIVE image database. Preprocessing: Green-band extraction was used to obtain better contrast, which facilitated better visualization of retinal blood vessels. A spatial highpass filter of mask-size 11 was applied. A histogram stretch was performed to enhance contrast. A median filter was applied to mitigate noise. At this point, the gray-scale image was converted to a binary image using a binary thresholding operation. Then, a NOT operation was performed by gray-level value inversion between 0 and 255. Postprocessing: The resulting image was AND-ed with its corresponding ring mask to remove the outer-ring (lens-edge) artifact. At this point, the above algorithm steps had extracted most of the major and minor vessels, with some intersections and bifurcations missing. Vessel segments were reintegrated using the Hough transform. Results: After applying the Hough transform, both the average peak SNR and the RMS error improved by 10%. Pratt's Figure of Merit (PFM) was decreased by 6%. Those averages were better than [1] by 10-30%. Conclusions: The new algorithm successfully preserved the details of smaller blood vessels and should prove successful as a segmentation step for automatically identifying diseases that affect retinal blood vessels.

Keywords: retinal images, retinal blood-vessel segmentation, fundus images, retinopathy, diabetic retinopathy

1. INTRODUCTION

About 4.1 million Americans suffer from diabetic retinopathy. Responsible for 11% of all cases, it is one of the major causes of blindness in Americans. Although, the symptoms are often not easily identifiable at the early non-proliferative stages, as the disease progresses, vascular damage ensues, leading to bleeding, cloudy vision and ultimately, blindness. Early detection of damaged vessels in retinal images can provide valuable information about the presence of disease, thereby helping to prevent blindness [2]. Timely treatment for diabetic retinopathy prevents severe vision loss in over 50% of eyes tested [3]. To help automatically diagnose various stages of the disease, a new blood-vessel-segmentation algorithm was developed to automatically segment retinal blood vessels [4, 5]. Using the algorithm in this study, the objective was to get better results than did the algorithm of a previous study, by more accurately segmenting the smaller vessels, keeping them intact, while minimizing more noise than in the previous study [1].

*bobleander@gmail.com; phone 1 618 650-2554; fax 1 618 6503374; http://www.ee.siue.edu/faculty/rleande

Medical Imaging 2010: Computer-Aided Diagnosis, edited by Nico Karssemeijer, Ronald M. Summers,
Proc. of SPIE Vol. 7624, 76243B · © 2010 SPIE · CCC code: 1605-7422/10/$18 · doi: 10.1117/12.844996

2. MATERIALS AND METHODS

2.1 Materials

Image Database: Twenty, 584 x 565-pixel, color retinal images and twenty of their corresponding, manually-segmented images were collected from the Digital Retinal Images for Vessel Extraction (DRIVE) retinal-image database. All human observers who manually segmented the vasculature were instructed and trained by an experienced ophthalmologist and asked to mark all pixels for which they were at least 70% certain that the pixels were vessel [6]. The first twenty images were used as a test set. The second twenty were used as a training set. Also provided in the database were ring masks for all the images to be used for masking out the outer-ring (edge) artifacts of the retinal images. Without the masks, the edges may have been factored in as vasculature, during calculations of segmentation metrics.

Software: Computer Vision and Image Processing Tools (CVIPtools) version 4.4, was used to implement the algorithm and to calculate SNR, RMS error and PFM – parameters that indicate the amount of match between the automatically-segmented and the manually-segmented images. The primary code implementing the segmentation algorithm was written in the C programming language and run in the Microsoft Visual Studio 2005 environment. The spatial highpass filter, as well as other functions, were called from CVIPtools by the C code.

2.2 Methods

Preprocessing: *Green-Band Extraction*: Because it contains the most pertinent amount of visual information and the most contrast, the green band (Band 2) was extracted from the images [7] (see Fig. 1). In order to match the one green band extracted from the retinal images, the green band of the outer-ring-mask image was extracted. Also, because the ring mask size did not exactly fit the ring size of its paired retinal image, a morphological filter having a size-11, circular structuring element was used to erode the edges of the mask.

Spatial Highpass Filtering: A spatial highpass filter of mask-size 11 was applied to the retinal image's green band [8, 9] (see Fig. 1). A mask of size 11 provided results which were similar to applying a frequency-domain, highpass filter, except without returning an output image whose size has been changed. *Enhancement*: A histogram stretch was applied to enhance image contrast, while a median filter mitigated salt-and-pepper noise. Regarding histogram-stretch parameters, the histogram clipping percentage was 0.025 percent at both ends of an image's histogram, while the stretch was done using the default minimum and maximum gray-level values of 0 and 255 [10]. After the histogram stretch operation, a median filter of mask-size 3 was used to remove residual noise.

Binary Thresholding: Images were then converted from gray-scale to binary, using a binary threshold value of 108 (see Fig. 1). 108 was the optimal threshold value derived from application feedback using the training images. Because the resultant image at this point had black segmentations with a white background, a NOT operation was performed to match the white vessels and black background of the observer-segmented images to which the processed images would be compared.

Postprocessing: *Ring-Artifact Removal:* The segmented image's outer-ring artifact was removed by logically AND-ing the image with the eroded ring mask (see Fig. 1). *Hough Transform*: At this point, a Hough transform was used to consummate vessel detection by reintegration of transections at intersections and bifurcations, as well as to eliminate noise points. Hough transform parameters for choosing pixels to be connected were the following: the minimum number of pixels required in a line ("Line Pixels") was 10; the range of angles along whose sides pixels were to be connected for constructing lines was 0 to 180 degrees, the minimum number of pixels allowed in a line segment (“Segment Pixels”) was 6, the minimum connecting distance between two segments was 2; the Hough space was quantized with a “Delta Length” of 1. The Hough transform outputs a binary-thresholded image for which the Threshold Level was left as “default.

Evaluation Methods: The algorithm-segmented images (before and after applying Hough transform) were compared with the observer-segmented images using three indices: peak SNR, RMS error and Pratt’s Figure of Merit (PFM).

3. ALGORITHM

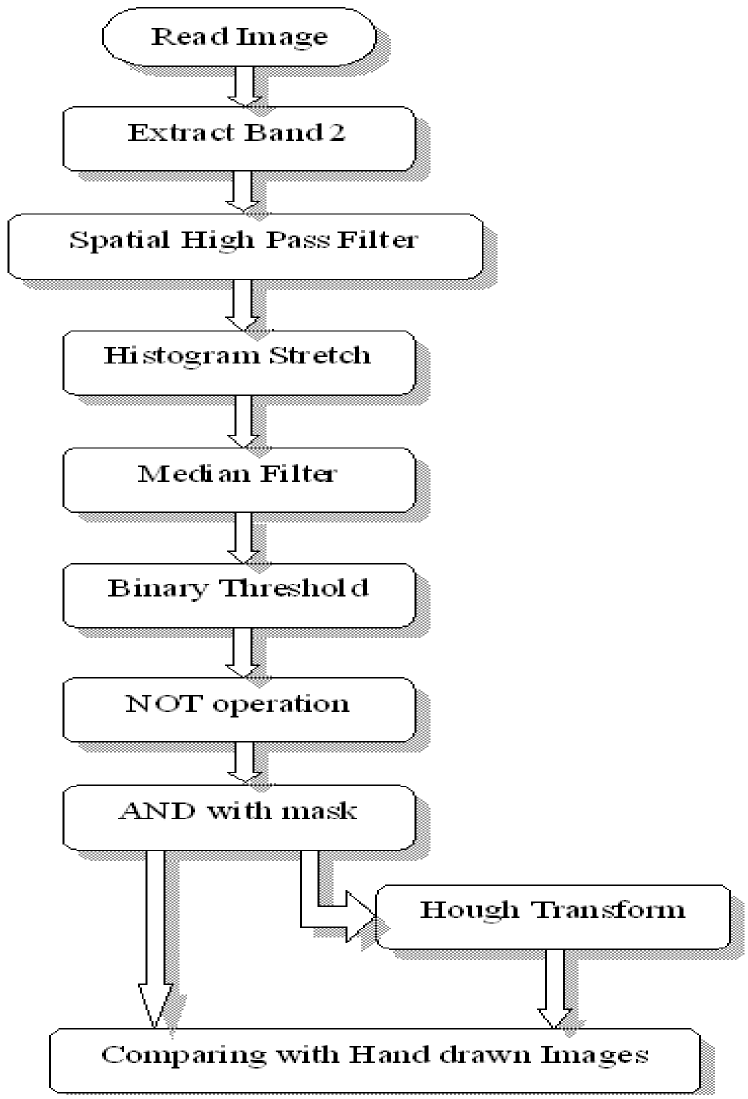

Fig. 1. Flow diagram for the vessel detection algorithm.

4. IMAGE PROCESSING RESULTS

Figures 2-4 show an original image from the STARE database, its segmentation by an ophthalmologist and a segmentation performed by an algorithm from the previous study [1]. Figures 5-7 show an original image from the DRIVE database, its segmentation by an ophthalmologist-trained observer and a segmentation performed by the new algorithm developed in this study. Figures 4 and 7 show that the segmentation capability of the new algorithm is an appreciable improvement over the capability of the algorithm in the previous study.

4.1 Images from the previous study

Fig. 2. Original Image from the STARE database, used in the previous study [1].

Fig. 3. Binary format of ophthalmologist's hand-drawn tracing of blood vessels in Fig 2.

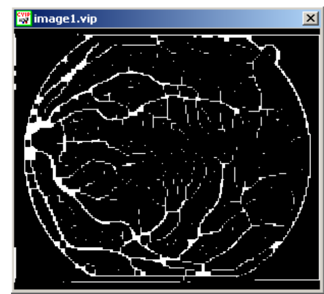

Fig. 4. Blood-Vessel-Segmentation-Algorithm 1's output image. Degree of match to the hand-drawn image in Fig. 3 using…
Pratt's Figure of Merit: 0.6506
Signal to Noise ratio: 12.14
RMS error: 63.027

4.2 Images from the present study

Fig. 5. Original Image from the DRIVE database used in this study.

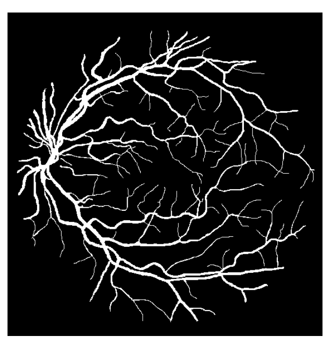

Fig. 6. Binary format of a human observer's hand-drawn tracing of blood vessels in Fig 5.

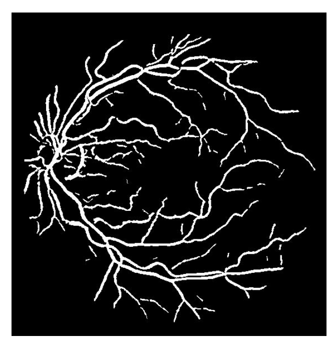

Fig. 7. Output Image of the new algorithm. Degree of match to the hand-drawn image in Fig. 6 using…
Pratt's figure of Merit: 0.9004
Signal to Noise ratio: 13.811
RMS error: 52.000

5. QUANTITATIVE RESULTS

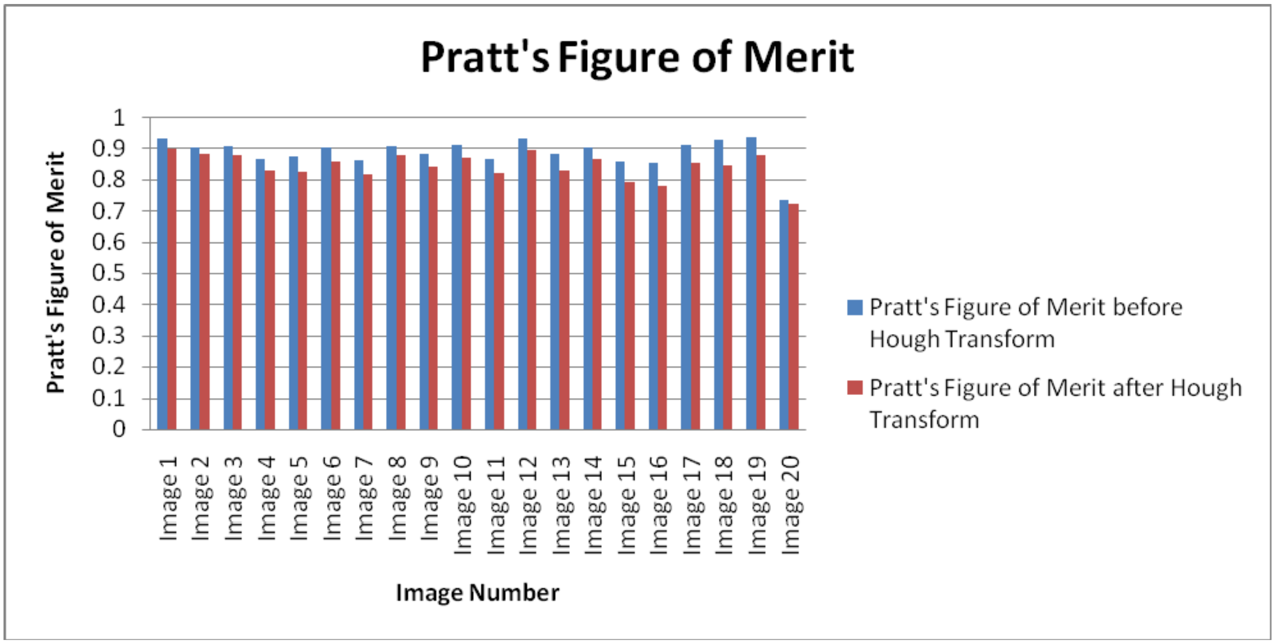

Fig. 8. Bar graph comparing Pratt's Figures of Merit (PFM) for output images using the new algorithm. Juxtaposed bars represent a comparison of the algorithm's effects, before and after use of the Hough transform. The figure shows that the use of Hough's transform decreased PFM.

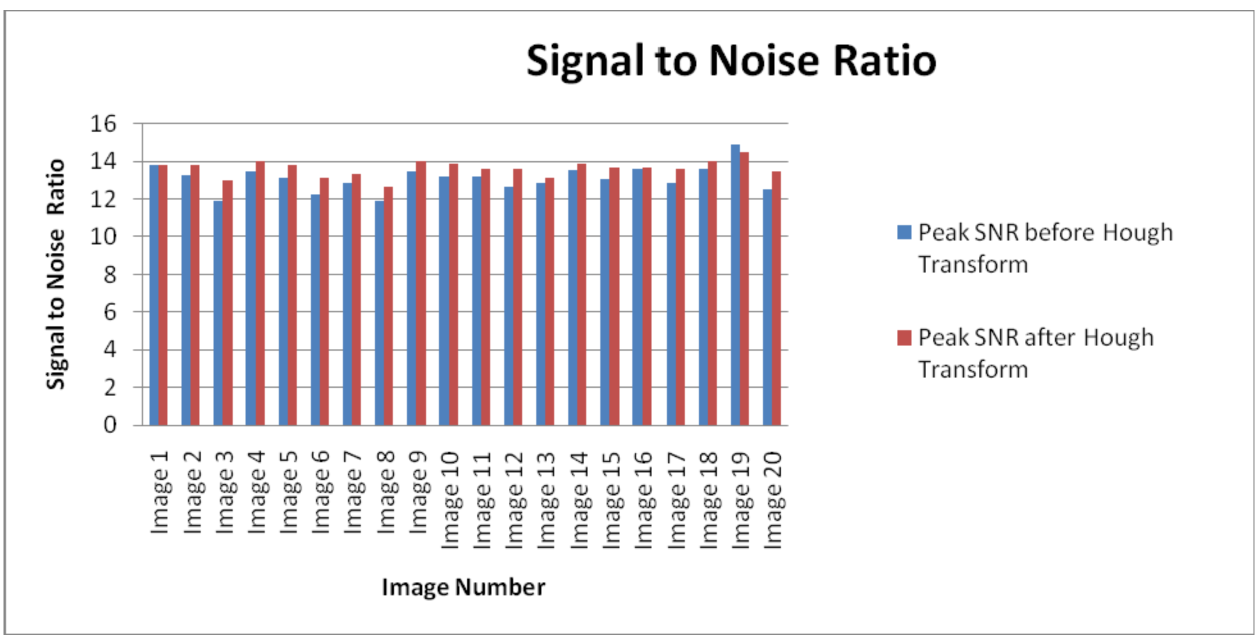

Fig. 9. Bar graph comparing peak Signal to Noise Ratio (SNR) for output images using the new algorithm. Juxtaposed bars represent a comparison of the algorithm's effects, before and after use of the Hough transform. The figure shows that the use of Hough's transform increased the SNR.

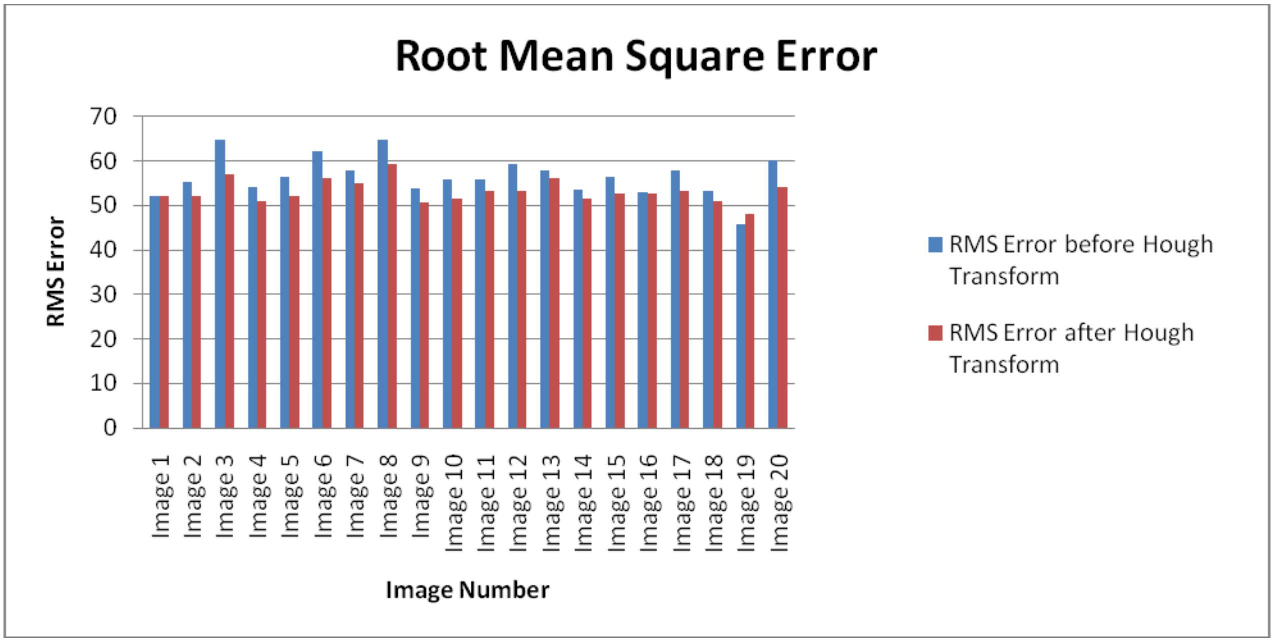

Fig. 10. Bar graph comparing the root mean square (RMS) error for output images using the new algorithm. Juxtaposed bars represent a comparison of the algorithm's effects, before and after use of the Hough transform. The figure shows that the use of Hough's transform decreased RMS error.

5. DISCUSSION

SNR, RMS error and PFM were better than the best algorithm in [1], by 10% to 30%. The algorithm components that segmented the blood vessels in effect, were the large mask of the highpass filter (size 11) and the binary threshold. A large mask size helped duplicate the effectiveness of an available frequency-domain filter, without changing the image size. After applying the Hough transform, there were improvements in SNR and RMS error by 10%. However, a decrease in PFM by 6% was a manifestation of the transform's partial success in reintegrating missing vessel intersections. Because a few of the smaller vessels were still missing, mismatches between the algorithm-segmented and the hand-drawn images occurred. Without these errors, SNR would be higher. Higher SNR and lower RMS error would be possible as well, if the ring masks were more perfectly-matched to their retinal images. During a few experiments using an adaptive histogram threshold, it was observed that better results could be achieved in SNR, RMS error and PFM.

6. SUMMARY

This study developed and evaluated a new algorithm for the automatic segmentation and detection of smaller blood vessels in fundus images. The principal component effecting the segmentation was a highpass filter. The algorithm's performance was appreciably better for segmenting both major and minor blood vessels than the best algorithm in [1]. More of the minor vessels were found with fewer intersections and bifurcations missing than in the previous study. Using a Hough transform to reintegrate and recover intersections and bifurcations of major vessels helped make appreciable improvements over the algorithm of the previous study. Using the new algorithm, although most of the major vessels' junctions could be recovered, some of the minor vessels' junctions could not.

7. CONCLUSION

The proposed algorithm was better able to successfully detect retinal blood vessels in fundus images, providing an improvement of 10%-30% over the best algorithm in [1]. The new algorithm in this study, successfully preserved many of the details of smaller blood vessels and should prove successful as a segmentation step for automatically identifying retinal diseases affecting blood vessel structural integrity.

8. REFERENCES

[1] LeAnder, R., Sushma, M.S., Mokkapati, S. and Umbaugh, S.E., "Comparison of Two Algorithms in the Automatic Segmentation of Blood Vessels in Fundus Images," Medical Imaging 2008: Computer-Aided Diagnosis, Proceedings of the SPIE, Volume 6915, 69153H-69153H-16 (2008).

[2] Meadows, M., "Saving your sight: Early detection is critical," FDA Consumer Magazine, (April 2002). http://www.fda.gov/fdac/features/2002/202_eyes.html

[3] Al-Rawi, M., Qutaishat, M. and Arrar, M., "An Improved Matched Filter for Blood Vessel Detection of Digital Retinal Images," Computers in Biology and Medicine 37, Vol. 37, Issue 2, 262 – 267 (February 2007).

[4] Patton, N., Aslam, T. M., MacGillivray, T., Deary, I.J., Dhillon, B., Eikelboom, R.H., Yogesan, K. and Constable, I.J., "Retinal Image Analysis: Concepts, Applications and Potential," Progress in Retinal and Eye Research 25, 99–127, (2006).

[5] Kirbas, C. and Quek, F., "A Review of Vessel Extraction Techniques and Algorithms," Wright State University, Dayton, Ohio, ACM Computing Surveys, Vol. 36, No. 2, (June 2004).

[6] Digital Retinal Images for Vessel Extraction: DRIVE Database: www.isi.uu.nl/Research/Databases/DRIVE/

[7] Rapantzikos, K., Zervakis, M. and Balas, K., "Detection and Segmentation of Drusen Deposits on Human Retina: Potential in the Diagnosis of Age-Related Macular Degeneration," Medical Image Analysis, Vol. 7, (March 2003).

[8] Sofka, M. and Stewart, C. V. , "Retinal Vessel Centerline Extraction using Multiscale Matched filters Confidence and Edge Measures," IEEE Transactions on Medical Imaging, Vol 25, No 12, 1531-1546, (2006).

[9] Chaudhuri, S., Chatterjee, S., Nelson, M., Katz, N. and Goldbaum, M., "Detection of Blood Vessels in Retinal Images Using Two Dimensional Matched Filters," Medical Imaging, IEEE, Volume 8, Issue 3, (Sep 1989).

[10] Umbaugh, S.E., [Computer Imaging: Digital Image Analysis and Processing], Boca Raton: CRC Press, (2005).

[11] Engelgau, M.M., Geiss, L.S. and Saaddine, J.B., "The Evolving Diabetes Burden in the United States," Ann Intern Med. 140:945-950, (2004).

[12] Teng, T., Lefley, M. and Claremont, D. "Progress towards Automatic Diabetic Ocular Screening: A Review of Image Analysis and Intelligent Systems for Diabetic Retinopathy," Medical and Biological Engineering and Computing, Vol. 40(1): 2-13, (2002).

[13] Abdel-Ghafar, R., Morris,T., Ritchings, T. and Wood, I., "Detection and Characterisation of the Optic Disk in Glaucoma and Diabetic Retinopathy," Proceedings of Medical Image Understanding and Analysis, (September 2004).

[14] Gonzalez, R.C., and Woods, R.E., [Digital Image Processing], Third Edition, Pearson/Prentice-Hall, 2008